Int J Adv Manuf Technol (2003) 21:79–83
Ownership and Copyright

The International Journal of Advanced Manufacturing Technology

Grinding of Aluminium-Based Metal Matrix Composites Reinforced with Al_2O_3 or SiC Particles

Z. W. Zhong
School of MPE, Nanyang Technological University, Singapore

This paper presents results obtained from the grinding of aluminium-based metal matrix composites reinforced with either aluminium oxide (Al_2O_3) or silicon carbide (SiC) particles using grinding wheels made of SiC in a vitrified matrix or diamond in a resin-bonded matrix. The study used grinding speeds of 1100–2200 m min^{-1}, a grinding depth of 15 μm for rough grinding and 0.1–1 μm for fine grinding, a crossfeed of 3 mm and 1 mm for rough and fine grinding, respectively, while maintaining a constant table feedrate of 20.8 m min^{-1}. Surface integrity of the ground surfaces and subsurfaces was analysed using a scanning electron microscope and a profilometer. Grinding using a 3000-grit diamond wheel at depths of cut of 1 μm and 0.5 μm produced ductile streaks on the Al_2O_3 particles and the SiC particles, respectively. There was almost no subsurface damage except for rare cracked particles when fine grinding with the diamond wheel.

Keywords: Al_2O_3 particle; Ductile streaks; Grinding; Metal matrix composites; SEM analysis; SiC particles; Surface integrity

1. Introduction

Aluminium-based metal matrix composites (MMCs) reinforced with ceramic particles are advanced materials known for their good damping properties, high specific strength, and high wear resistance. Methods to produce these composites and studies on their mechanical properties have gained popularity [1]. MMCs are increasingly used in astronautic, automobile, and military industries. In addition, the sporting goods industry has also been in the forefront of MMCs development capitalising on the materials' high specific properties. There is also a growing interest in the shipping industry [2].

Reports on machining of aluminium-based MMCs reinforced with ceramic particles [3–6] are still scarce. Despite many advantages, full implementation of MMCs is cost-prohibitive. This is partially due to the poor machinability of the materials. Although near-net-shape MMC components can be produced, final finishing is still required for obtaining designed final dimensions and required surface finish. Significant cost and fabrication problems, including machining, must be overcome for the successful application of these composites. Surface finish and surface integrity are important for surface sensitive parts subjected to fatigue. Subsurface damage due to the machining of MMCs results from conventional and unconventional processes, therefore, finishing processes such as grinding are used to improve the surface integrity of machined MMCs [7,8].

Work on grinding silicon and germanium revealed that ductile chips could be obtained by properly controlling the depth of cut [9]. A model for the critical depth associated with ductile-mode machining has been proposed [10]. It was reported that by having a critical depth of cut and with flattened grains slightly protruding from the surface of the grinding wheel, flawless machining, free of brittle fracture, was possible [11]. Evidence of plastic flow with aluminium oxidide (Al_2O_3), silicon carbide (SiC), and silicon nitride (Si_3N_4) was shown and a model based on the combination of two theories was proposed [12]. A hundred per cent ductile-mode mirror grinding of SiC could be achieved by using a non-ultraprecision machine with a 1 μm in-feed (depth of grinding) which would produce large mirror surfaces comparable to well-polished mirrors [13,14].

However, reports on the ductile-mode machining of aluminium-based MMCs reinforced with ceramic particles are still very scarce. Therefore, further studies on the ductile-mode machining of these materials to obtain damage-free surfaces are required for the application of these materials. This paper presents results obtained from the grinding of aluminium-based MMCs reinforced with either SiC or Al_2O_3 particles. The issues discussed are surface roughness, grinding force, type and size of the abrasives, grinding conditions, ductile streaks on Al_2O_3 and SiC particles and the consequential subsurface integrity.

2. Experiments

The details of the ground MMC specimens 2618/Al_2O_3/10p (10 vol% Al_2O_3), 2618/Al_2O_3/20p (20 vol% Al_2O_3), and

Correspondence and offprint requests to: Dr Z. W. Zhong, School of Mechanical and Production Engineering, Nanyang Technical University, 50 Nanyang Avenue, Singapore 639798 E-mail: mzwzhong@ntu.edu.sg

Table 1. The metal matrix composites machined.

Material	$2618/Al_2O_3/10p$	$2618/Al_2O_3/20p$	A359/SiC/10p-T6
Matrix	2618 aluminium alloy	2618 aluminium alloy	A359 aluminium alloy: 8.96 wt% Si, 0.18 Fe, 0.53 Mg, balance Al
Reinforcement	10 vol% Al_2O_3 particulate particle size: 9.3 μm	20 vol% Al_2O_3 particulate particle size: 21 μm	10 vol% SiC particulate mean 13 μm, aspect ratio 1.5:1 97% particle <25 μm 6% <5 μm
Process	Extrusion at 420–430°C Extrusion ratio: 20:1 Extrusion speed: 3 m min^{-1}	Extrusion at 420–430°C Extrusion ratio: 20:1 Extrusion speed: 3 m min^{-1}	Pouring temperature: 700–710°C Hot isostatic pressing by heating at 550°C, isostatically pressed at 150 MPa, oven-cooled to 300°C, then air-cooled Solution heat-treated at 540°C, water quenched, peak aged at 155°C

A359/SiC/10p-T6 (10 vol% SiC) are shown in Table 1. The MMCs are cast aluminium alloys reinforced with Al_2O_3 or SiC particles. A359/SiC/10p-T6 was hot-isostatically pressed and aged to enhance the matrix properties.

Table 2 shows the details of the grinding conditions and the grinding wheels used. A resin-bonded diamond grinding wheel was used to fine grind the MMC specimens at low, medium, and high grinding speeds, respectively. The grit size was 3000 (5 μm average grain size). Some $2618/Al_2O_3/10p$ and $2618/Al_2O_3/20p$ workpieces were also rough ground with an 80-grit vitrified-bond SiC grinding wheel at low, medium, and high grinding speeds, respectively.

Grinding experiments were carried out on an Okamoto precision surface-grinding machine. An inverter was attached to the machine spindle motor so that the main spindle of the machine was capable of changing speed. A dynamometer was mounted on the table of the grinding machine to measure the grinding forces. The dynamometer was connected to charge amplifiers, and the measured grinding forces were recorded using a chart recorder. The grinding force reported here is the force perpendicular to a ground surface.

A SiC wheel mounted on a brake-controlled trueing device and a single diamond dresser were used for trueing the grinding wheels. SiC and WA dressing sticks were used for dressing the SiC and diamond grinding wheels, respectively. Dressing was carried out before every grinding experiment.

The surface roughness of the ground MMCs was measured in the direction perpendicular to the grinding direction using a profilometer. The cut-off was 0.8 mm and evaluation length was 4 mm. The average value was calculated from three values measured on each ground surface.

Surface integrity of the machined surfaces and subsurface damage were assessed using a scanning electron microscope (SEM). The samples were observed in the as-machined condition. Some samples were observed again after being etched in Keller's etchant (190 ml water, 5 ml nitric acid, 3 ml hydrochloric acid, 2 ml fluoric acid) to dissolve the smeared aluminium on the surfaces. Selected samples were sectioned, moulded, hand ground, polished, and then etched to show the microstructure at the subsurface.

Table 2. Grinding conditions and grinding wheels used.

Attributes		Rough grinding of $2618/Al_2O_3/10p$	Fine grinding of $2618/Al_2O_3/20p$	Finding grinding of A359/SiC/10p-T6
Grinding wheel	Grain	Green SiC	Diamond	Diamond
	Grit size	80	3000	3000
	Bond	Vitrified bond	Resin bond	Resin bond
	Diameter (mm)	350	350	350
	Width (mm)	38	10	10
Dressing stick	Grain	Green SiC	WA	WA
	Grit size	60	320	320
Grinding speed	Low (m min^{-1})	1100	1100	1100
	Medium (m min^{-1})	1650	1650	–
	High (m min^{-1})	2200	2200	–
	Depth of cut (μm)	15	1	0.1, 0.2, 0.5, 1
	Feedrate (m min^{-1})	20.8	20.8	20.8
	Cross-feed (mm)	3	1	1

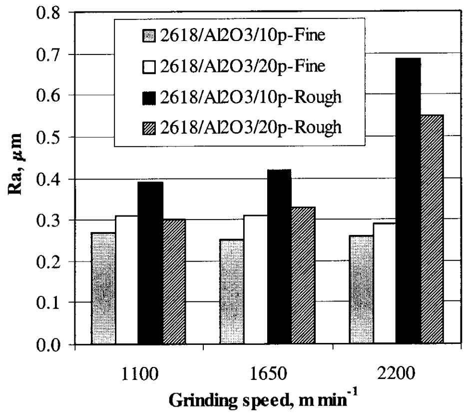

Fig. 1. Surface roughness of ground 2618/Al_2O_3/10p and 2618/Al_2O_3/20p. Rough grinding (80-grit SiC wheel; depth of cut: 15 μm; cross-feed: 3 mm). Fine grinding (3000-grit diamond wheel; depth of cut: 1 μm; cross-feed: 1 mm).

3. Results and Discussion

The surface roughness values of rough- and fine-ground 2618/Al_2O_3/10p (10 vol% Al_2O_3) and 2618/Al_2O_3/20p (20 vol% Al_2O_3) are shown in Fig. 1. Values of the maximum grinding force measured during the rough and fine grinding experiments are shown in Fig. 2. Figures 3 and 4 show the top and cross-section of rough-ground surfaces, whereas Figs 5 to 8 show those of fine-ground surfaces.

As shown in Fig. 1, the surface finish *Ra* of the fine-ground 2618/Al_2O_3/10p (10 vol% Al_2O_3) was better than that of fine-ground 2618/Al_2O_3/20p (20 vol% Al_2O_3). However, the *Ra* of rough-ground 2618/Al_2O_3/10p was worse than that of rough-ground 2618/Al_2O_3/20p. This demonstrates the effects of the Al_2O_3 particles of the ground samples on the performance of the SiC and diamond grinding wheels. For the rough-ground samples, the *Ra* values were scattered in the range 0.15–0.70 μm. A narrower range of 0.20–0.35 μm was achieved for the fine-ground samples. Surfaces ground by the 80-grit SiC wheel at speeds of 1100 and 1650 m min^{-1} at depth of cut of 15 μm had roughness values close to those of surfaces produced by the 3000-grit diamond wheel at depth of cut of 1 μm. This

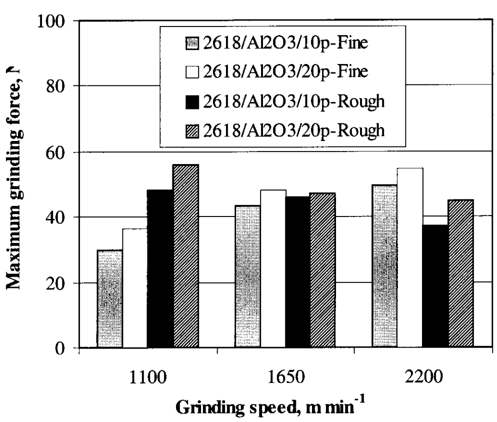

Fig. 2. Forces for grinding 2618/Al_2O_3/10p and 2618/Al_2O_3/20p. Conditions as Fig. 1.

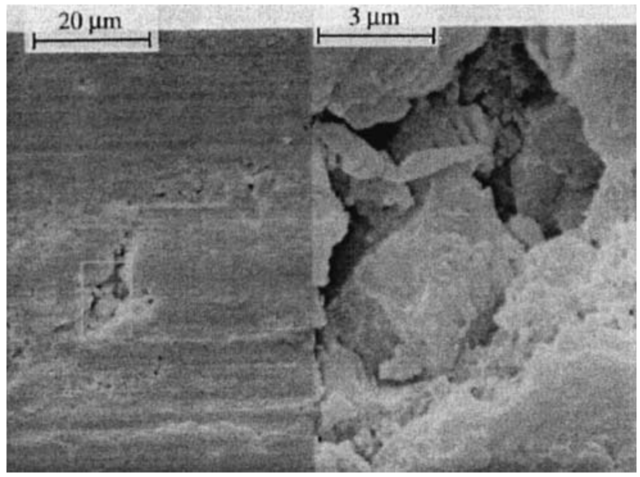

Fig. 3. SEM micrograph of ground 2618/Al_2O_3/20p surface. Rough grinding (80-grit vitrified-bond SiC wheel; grinding speed: 2200 m min^{-1}; depth of cut: 15 μm; cross-feed: 3 mm; feedrate: 20.8 m min^{-1}).

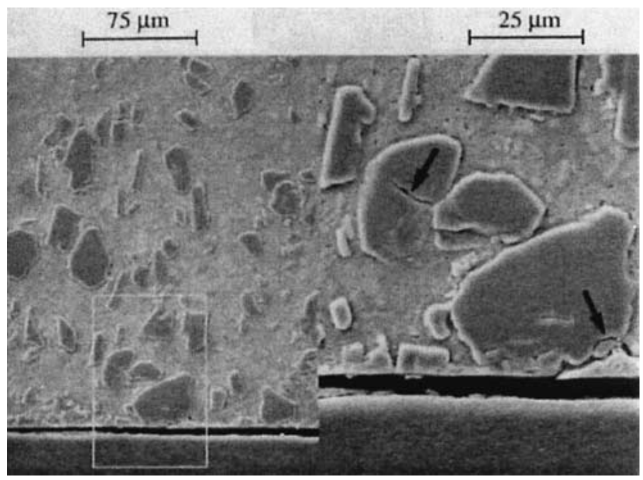

Fig. 4. Subsurface of ground 2618/Al_2O_3/20p. The arrows show cracks of commonly found Al_2O_3 particles. Rough grinding, conditions as Fig. 3.

was due to the smearing of the aluminium matrix. Smearing of aluminium on the ground surfaces was seen for the rough grinding, but was negligible for the fine grinding because all the Al_2O_3 particles of the ground surfaces were clearly visible when observed with the SEM.

The maximum grinding force decreased with increasing grinding speed for rough grinding, but increased with increasing grinding speed for fine grinding. This could be due to several reasons such as the different abrasives, grit sizes and depths of cut used for the rough- and fine-grinding experiments, and the thermal-induced softened matrix at high speeds for rough grinding, etc. For example, because the depth of cut was 15 μm for rough grinding of the Al_2O_3 particles (particle size: 9.3 or 21 μm), more heat was generated in the deformation zone. This softened the matrix at the higher grinding speed and lowered the grinding force component perpendicular to the ground surface. In the case of fine grinding, because the depth

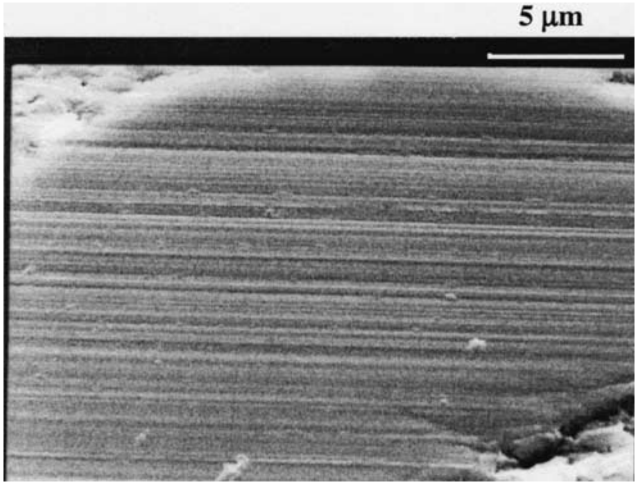

Fig. 5. SEM micrograph of ground 2618/Al_2O_3/20p surface. Fine grinding (3000-grit resin-bond diamond wheel; grinding speed: 1100 m min^{-1}; depth of cut: 1 μm; cross-feed: 1 mm; feedrate: 20.8 m min^{-1}).

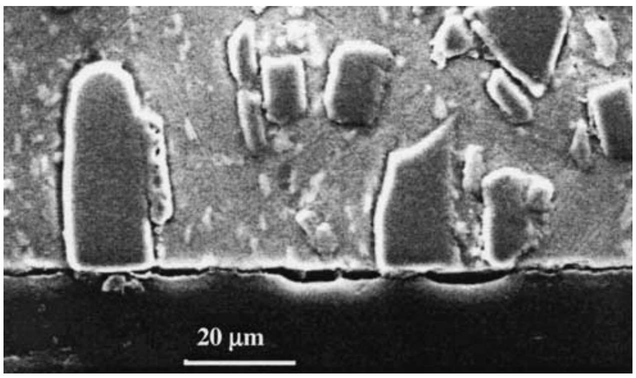

Fig. 6. Subsurface of ground 2618/Al_2O_3/20p. Find grinding, conditions as Fig. 5.

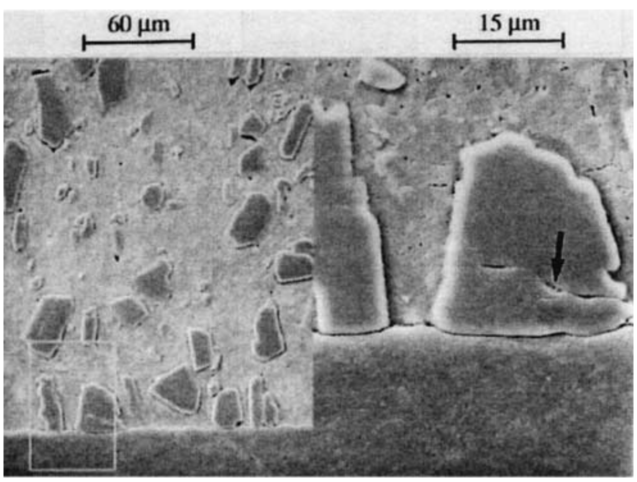

Fig. 7. Subsurface of ground 2618/Al_2O_3/20p. The arrow shows the rare crack of an Al_2O_3 particle. Fine grinding, conditions as Fig. 5, but grinding speed: 2200 m min^{-1}.

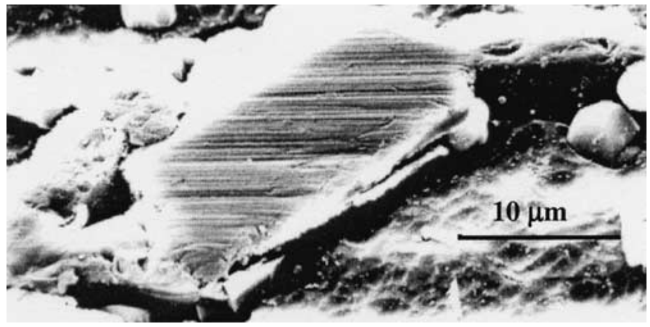

Fig. 8. SEM micrograph of ground A359/SiC/10p-T6 surface. Fine grinding, conditions as Fig. 5, but depth of cut: 0.5 μm.

of cut was 1 μm, the thermal effect was presumably negligible. Further investigation is required to understand better the micromachining mechanism of both the soft matrix and the hard, brittle particles at the same time. However, from Fig. 2, it can be seen clearly that the grinding force required for grinding the MMCs with 20 vol% Al_2O_3 particles is usually higher than that for grinding the MMCs with 10 vol% Al_2O_3 particles.

Figures 3 and 4 show that cracks in the Al_2O_3 particles occur at the surface and under the rough ground surfaces. As mentioned above, surfaces rough ground at speeds of 1100 and 1650 m min^{-1} have roughness values close to those of fine-ground surfaces. However, SEM pictures show that the surface topographies of the rough- and fine-ground surfaces having very similar surface roughness values, are significantly different. No Al_2O_3 particles were seen on the rough-ground surfaces, except some small holes showing fractured Al_2O_3 particles, as shown in Fig. 3. Almost the whole surfaces were smeared with the soft aluminium matrix. Some of aluminium chips were back-transferred onto the top of the surfaces.

SiC wheels are much cheaper than diamond wheels. The cost ratio is roughly 1:10–20. Because the depth of cut and cross-feed used were 15 and 3 times those for fine grinding, using a depth of cut 1 μm, respectively, the specific material removal rate was 45 times that of the fine grinding using the diamond wheel. The grinding time was also much shorter than for fine grinding. Hence, the potential of using SiC wheels, at least for rough grinding, is high. Rough grinding parameters and dressing frequency should be optimised to make rough grinding using SiC wheels more attractive.

As shown in Fig. 5, grinding of 2618/Al_2O_3/20p (20 vol% Al_2O_3) using the fine-grit diamond wheel at 1 μm in-feed (depth of grinding) produced visible ductile streaks on the Al_2O_3 particles. Both the matrix and the Al_2O_3 particles were removed by micromachining because the ductile grinding marks were clearly seen on the Al_2O_3 particles. There were no cracks or defects found on the ground surfaces. There was almost no subsurface damage as shown in Fig. 6, except a very rare cracked particle as shown in Fig. 7.

The diamond wheel also produced A359/SiC/10p-T6 (10 vol% SiC) surfaces with few SiC-particle-related defects. A very thin smearing layer of aluminium and partially hidden SiC particles was observed on the ground surfaces. When lightly etched with Keller's etchant, the ductile-mode ground surfaces of the SiC particles can be seen. As shown in Fig. 8, with a depth of cut of 0.5 μm, ductile-mode grinding of SiC particles was observed.

4. Summary

Diamond grinding experiments were performed on aluminium-based MMCs reinforced with SiC or Al_2O_3 particles. The potential of using SiC wheels at least for rough grinding of alumina/aluminium composites is high, because SiC grains are harder than the Al_2O_3 reinforcing particles and are much less expensive than diamond grains. Rough grinding with a SiC wheel followed by fine grinding with a fine-grit diamond wheel is recommended for the grinding of alumina/aluminium composites. Grinding using a 3000-grit diamond wheel at depths of cut of 1 μm and 0.5 μm produced many ductile streaks on the Al_2O_3 particles and the SiC particles, respectively.

Acknowledgement

The author would like to thank Dr N. P. Hung for the MMCs and for his cooperation.

References

1. M. J. Tan, L. H. Koh, K. A. Khor, F. Y. C. Boey, Y. Murakoshi and T. Sano, "Discontinuous reinforcements in extruded aluminium–lithium matrix composite", Journal of Materials Processing Technology, 37, pp. 391–403, 1993.
2. N. L. Loh, "MMCs current stage development and potential/anticipated applications in the future", Proceedings of the International Symposium on High Performance Metal Matrix Composites, Japan, pp. 11–12, 1994.
3. N. Tomac and K. Tonnessen, "Machinability of particulate aluminum matrix composites", Annals CIRP, 41(1), pp. 55–58, 1992.
4. P. Chen, "High-performance machining of SiC whisker-reinforced aluminum composite by self-propelled rotary tools", Annals CIRP, 41(1), pp. 59–62, 1992.
5. W. Konig, L. Cronjager, G. Spur, H. K. Tonshoff, M. Vigneau and W. J. Zdeblick, "Machining of new materials", Annals CIRP, 39(2), pp. 673–681, 1990.
6. Z. J. Yuan, L. Geng and S. Dong, "Ultraprecision machining of SiCw/Al composites", Annals CIRP, 42(1), pp. 107–109, 1993.
7. N. P. Hung, Z. W. Zhong and C. H. Zhong, "Grindability of metal matrix composites", Proceedings of the Fourth Conference on Composites Engineering, Hawaii, pp. 459–460, 1997.
8. N. P. Hung, Z. W. Zhong and C. H. Zhong, "Grinding of metal matrix composites reinforced with silicon carbide particles", Journal of Materials and Manufacturing Processes, 12 (6), pp. 1075–1091, 1997.
9. P. N. Blake, "Ductile-regime turning of germanium and silicon", PhD thesis, North Carolina State University, Rayleigh, NC, 1988.
10. T. G. Bifano, T. A. Dow and R. O. Scattergood, "Ductile-regime grinding of brittle materials: experimental results and the development of a model", Advances in Fabrication and Metrology for Optics and Large Optics, SPIE 966, pp. 108–115, 1988.
11. W. Konig and V. Sinhoff, "Ductile grinding of ultra-precise aspherical optical lenses", SPIE, Lens and Optical Systems Design, pp. 778–788, 1992.
12. K. Kitajima, G. Q. Cai, N. Kumagai, Y. Tanaka and H. W. Zheng, "Study on mechanism of ceramic grinding", Annals CIRP, 41(1), pp. 367–371, 1992.
13. Z. W. Zhong, "New grinding methods for aspheric mirrors with large curvature radii", Annals CIRP, 41(1), pp. 335–338, 1992.
14. Z. W. Zhong and V. C. Venkatesh, "Generation of parabolic and toroidal surfaces on silicon and silicon based compounds using diamond cup grinding wheels", Annals CIRP, 43(1), pp. 323–326, 1994.